Electronic Supplementary Material (ESI) for Materials Advances.

Supporting Information

Optimization of SnO_2 Electron Transport Layer for Efficient Planar Perovskite Solar Cells with Very Low Hysteresis

Abed Alrhman Eliwi[a†], Mahdi Malekshahi Byranvand[a,b,c,d†*], Paul Fassl[a,b*], Motiur Rahman Khan[a], Ihteaz Muhaimeen Hossain[a,b], Markus Frericks[e,f], Simon Ternes[a,b], Tobias Abzieher[a], Jonas A. Schwenzer[a], Thomas Mayer,[e] Jan P. Hofmann,[e] Bryce S. Richards[a,b], Uli Lemmer[a,b], Michael Saliba[c,d] and Ulrich W. Paetzold[a,b*]

[a]Light Technology Institute, Karlsruhe Institute of Technology, Engesserstrasse 13, 76131 Karlsruhe, Germany.

[b]Institute of Microstructure Technology, Karlsruhe Institute of Technology, Hermann-von-Helmholtz-Platz 1, 76344 Eggenstein-Leopoldshafen, Germany. E-mail: paul.fassl@kit.edu, ulrich.paetzold@kit.edu

[c]Institute for Photovoltaics (ipv), University of Stuttgart, Stuttgart, Germany. E-mail: mahdi.malekshahi@ipv.uni-stuttgart.de

[d]IEK-5 Photovoltaik, Forschungszentrum Jülich, Jülich, Germany.

[e]Surface Science Laboratory, Department of Materials and Earth Sciences, Technical University of Darmstadt, Otto-Berndt-Straße 3, 64287 Darmstadt, Germany.

[f]InnovationLab GmbH, Speyerer Straße 4, 69115 Heidelberg, Germany.

† These authors contributed equally to this work.

Experimental Section

Perovskite solar cells (PSCs) fabrication: The *n-i-p* architecture perovskite solar cells (PSCs) were fabricated: glass substrate, indium tin oxide (ITO)/ SnO_2 electron transport layer (ETL) /double-cation perovskite absorber layer/2,2′,7,7′-tetrakis(N, N′-di-p-methoxy phenylamine)-9,9′-spirobifluorene (Spiro-OMeTAD) hole transport layer (HTL)/Au back electrode.

Electron transport layers (ETLs) fabrication: Patterned ITO-coated glass substrates with a sheet resistance of 15 Ω sq^{-1} were consecutively cleaned in an ultrasonic bath containing eliminator, acetone (Sigma-Aldrich, 98%), and isopropyl alcohol (IPA, Sigma-Aldrich, 98%) for 10 min each step, and then dried by an N_2 flow, followed by oxygen plasma cleaning at 100 W power for 3 min. For preparing the SnO_2 compact layers (**c-SnO_2**), Tin chloride solution was spin coated on ITO substrates (2000 rpm for 60 s), followed by an annealing step at 200 °C for 30 min. The various concentrations of Tin chloride solutions (0.01 M, 0.02 M and 0.05M) of Tin chloride solution were prepared by dissolving the $SnCl_2.H_2O$ powder (Sigma-Aldrich, 98%) in absolute ethanol (Sigma-Aldrich, 99.9%). Afterward, for fabrication of **c(Li)-SnO_2** layers, Li-TFSI solution was spin coated (3000 rpm for 60 s) on **c-SnO_2** layers followed by an annealing step at 300 °C for 30 min. It should be noted that various annealing temperature (250 °C, 300 °C, 350 °C) were tested to find the optimum condition. The various concentrations of Li-TFSI solution (0.01 M, 0.5 M and 0.1 M) were prepared by dissolving Li-TFSI powder (Sigma-Aldrich, 99.95%) in anhydrous acetonitrile (ACN, Sigma-Aldrich, 99.8%). Finally, for fabrication of **c(Li)-NP-SnO_2** layers, a commercial potassium-containing colloidal solution of SnO_2 nanoparticles (NP-SnO_2) (Alfa Aesar, tin(IV) oxide, 15% in H_2O colloidal dispersion, product number 44592) with various concentrations (1 wt%, 1.5 wt% and 2 wt% diluted in DI water) was deposited on **c(Li)-SnO_2** layers at 4000 rpm for 30 s followed by an annealing step at 250 °C for 30 min. It should be noted

that after deposition of each layer of the ETLs, to improve the wettability, the surface was treated with oxygen plasma at 30 W power for 1 min.

Perovskite thin film fabrication: Double-cations perovskite ($(FAPbI_3)_{0.97}(MAPbBr_3)_{0.03}$) thin films were deposited on top of the ETLs substrates via a two-step spin coating process. At the first step, lead iodide (PbI_2) solution was spin coated at 1500 rpm for 30 s under N_2 atmosphere (in glove box) followed by an annealing step at 70 °C for 1 min. It should be noted that before deposition of the PbI_2 layer, all ETLs substrates were treated by oxygen plasma cleaning at 30 W power for 1 min. The 1.3M PbI_2 precursor solution was prepared by dissolving PbI_2 powder (Sigma-Aldrich, 99.999%) in the 9.5:0.5 (volume ratio) solvent mixture of N,N-dimethylformamide (DMF, Sigma Aldrich, anhydrous, 99.8%) and dimethyl sulfoxide (DMSO, Sigma Aldrich, anhydrous, ≥99.9%). At the second step, a solution of 60 mg formamidinium iodide (FAI, GreatCell Solar), 6 mg methylammonium bromide (MABr, GreatCell Solar) and 6 mg methylammonium chloride (MACl, Lumtec) in 1 ml IPA were spin coated onto the PbI_2 thin films at 1300 rpm for 30 s followed by a thermal annealing step at 150 °C for 15 min in ambient conditions (30–40% humidity). Afterward, HTL solution consisting of 79.8 mg of Spiro-OMeTAD (Luminescence Technology), 28.5 µL of 4-tert-butylpyridine (TBP, Sigma-Aldrich), 17.5 µL of Li-TFSI solution (520 mg in 100 µL ACN) in 1 mL chlorobenzene was spin coated on perovskite thin films at 4000 rpm for 30 s. For oxygen doping, the samples were kept overnight in a dry box for 12 h. Finally, the samples were transferred to the high-vacuum evaporator, where gold was deposited as the top anode (60 nm) through a shadow mask to define the active area to 0.105 cm^2.

Sample Characterization—UV-Vis spectrophotometry: The transmittance, reflectance and absorption spectra of the ETLs and perovskite thin films and EQE spectra of the PSCs were

measured with a Bentham PVE300 photovoltaic service characterization system by illuminating the solar cell with modulated monochromatic light.

Sample Characterization—X-Ray diffraction (XRD): The crystallinity of the perovskite thin films was examined by an XRD (D2Phaser from Bruker) machine with Cu-Kα radiation (λ = 1.5405 Å) in Bragg–Brentano configuration using a LynxEye detector.

Sample Characterization—Atomic force microscopy (AFM): AFM was performed on a Dimension Icon AFM (Bruker, Karlsruhe, Germany) in standard tapping mode in air. Cantilevers of type HQ/NSC15/AI BS (MikroMasch) were used with a nominal force constant of 40 N m−1 and a resonance frequency of 325 kHz. The roughness values were calculated using NanoScope Analysis 1.9.

Sample Characterization—Scanning electron microscopy (SEM): The surface of the perovskite layers was measured with Hitachi S4800 field emission scanning electron microscopy and cross-sectional SEM was measured with a scanning electron microscope (Zeiss LEO1530) with an in-lens detector and an aperture size of 20 µm.

Sample Characterization—Photoluminescence quantum efficiency and time resolved photoluminescence measurements: Integrating sphere measurements were carried out using an integrating sphere (LabSphere, 15 cm diameter) in ambient air (relative humidity < 40%). A green laser (LD-515-10MG from Roithner Lasertechnik) was directed into the sphere *via* a small entrance port (4 mm diameter). An optical fiber was used to collect the emission from the exit port of the integrating sphere and transfer it to the spectrometer (AvaSpec-ULS2048x64TEC from Avantes). The spectral response was calibrated using a calibration lamp (HL-3plus-INT-Cal from Ocean Optics). All raw measured spectra were recalculated to give power spectrums. The photoluminescence quantum efficiency (Q_e^{lum}) was determined using the method described by de

Mello *et al*.[1] The samples were placed at an angle of ~15° with respect to the laser beam to avoid specular reflectance towards the entrance port. The power density absorbed by the sample was calculated based on the laser intensity shone into the sphere (tracked by a power meter using a 90/10 beam splitter), the laser spot size (4.5 mm^2) and the absorptance *A* of the samples. The power density for the intensity dependent measurements was adjusted by a filter wheel (Thorlabs). The radiative limit of the V_{OC} ($V_{OC\text{-}rad}$) was determined as described by Kirchartz et al.[2] and the implied V_{OC} ($V_{OC\text{-}imp}$) (Fig. 5a) was calculated using $V_{OC,imp} = V_{OC,rad} + \frac{kT}{q} \cdot \ln Q_e^{lum}$.

Time-resolved photoluminescence (TRPL) measurements was carried out by a custom-built setup. A pulsed laser of 532 nm with a repetition rate of 1 kHz and a pulse width of 0.8 ns was used for the excitation of the samples. All measurements were performed with a pump fluence of ~400 nJ/cm^2. The photoluminescence was captured using an ACTON spectrometer and a CCD camera PIMAX512 at room temperature. All PL measurements were carried out in air.

Sample Characterization—X-ray photoelectron spectroscopy (XPS): ETLs were characterized by XPS using a PHI Versa Probe 5000 with monochromatic Al-Kα radiation (hv = 1486.6 eV). The take off angle was 90°. Survey spectra were measured with a pass energy of 187.85 eV and core level spectra at 11.75 eV. From detailed core level spectra, a Shirley-type background has been subtracted[3,4] and the spectra were binding energy referenced to calibration measurements of Ar^+-ion etched Ag foil. The base pressure in the analysis chamber was in the range of 10^{-9} mbar.

Sample Characterization—Current-Density–Voltage (J–V) Measurements: The solar cells were characterized using 21 Channel LED Solar Simulator (Wavelabs Solar Metrology Systems) inside a nitrogen filled glove box with a simulated AM1.5G spectrum calibrated 100 mW cm^{-2} using a KG5 short pass-filtered silicon reference solar cell. The *J–V* characteristics were measured in both reverse and forward direction with a constant scan rate of circa 0.6 V s^{-1} (Keithley 2400 source

measurement unit). The MPP was tracked by using a perturb-and-observe method. It should be mentioned that a 0.078 cm^2 mask was used to keep the active area constant for all solar cells throughout the measurements. The temperature of the solar cells set to 25 °C by an actively controlled Peltier element during *J–V* analyses and MPP tracking.

Sample Characterization—EIS and Photo-CELIV Measurements: The electrochemical impedance spectroscopy (EIS) and photogenerated charge extraction by linearly increasing voltage (Photo-CELIV) measurements were performed on Paios (Fluxim AG)- platform for all-in-one-characterization of solar cells and OLEDs. A white LED (Cree XP-G) was used for the illumination. The EIS measurements were performed under open circuit voltage with the perturbation AC voltage amplitude of 50 mV in a frequency range 1Hz-1M Hz.

For the Photo-CELIV measurements, a 100 µs light pulse illumination was used to generate the charge carriers in the perovskite. Shortly after the illumination, charge extraction was assisted by negative voltage with a ramp rate of 0.04 V/µs. For the mobility calculation, following formula was used $\mu = \frac{2d^2}{3At_{max}{}^2(1 + 0.36\Delta J/J_0)}$, where d is the thickness of the active layer, A is the ramp rate of extraction voltage, t_{max} is the location of the current maxima, J_0 is the displacement current plateau and ΔJ is the current increment from the plateau as shown in the following schematic of photo-CELIV signal.

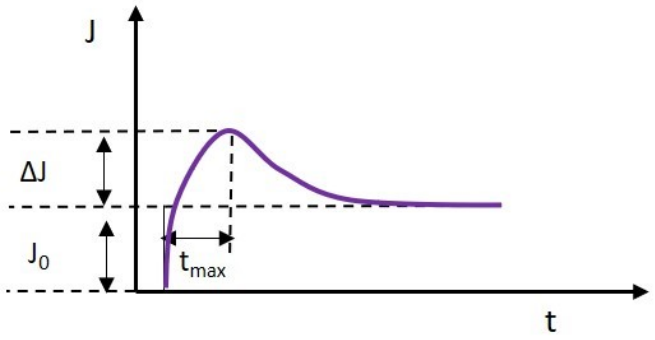

Supplementary Figures and Tables

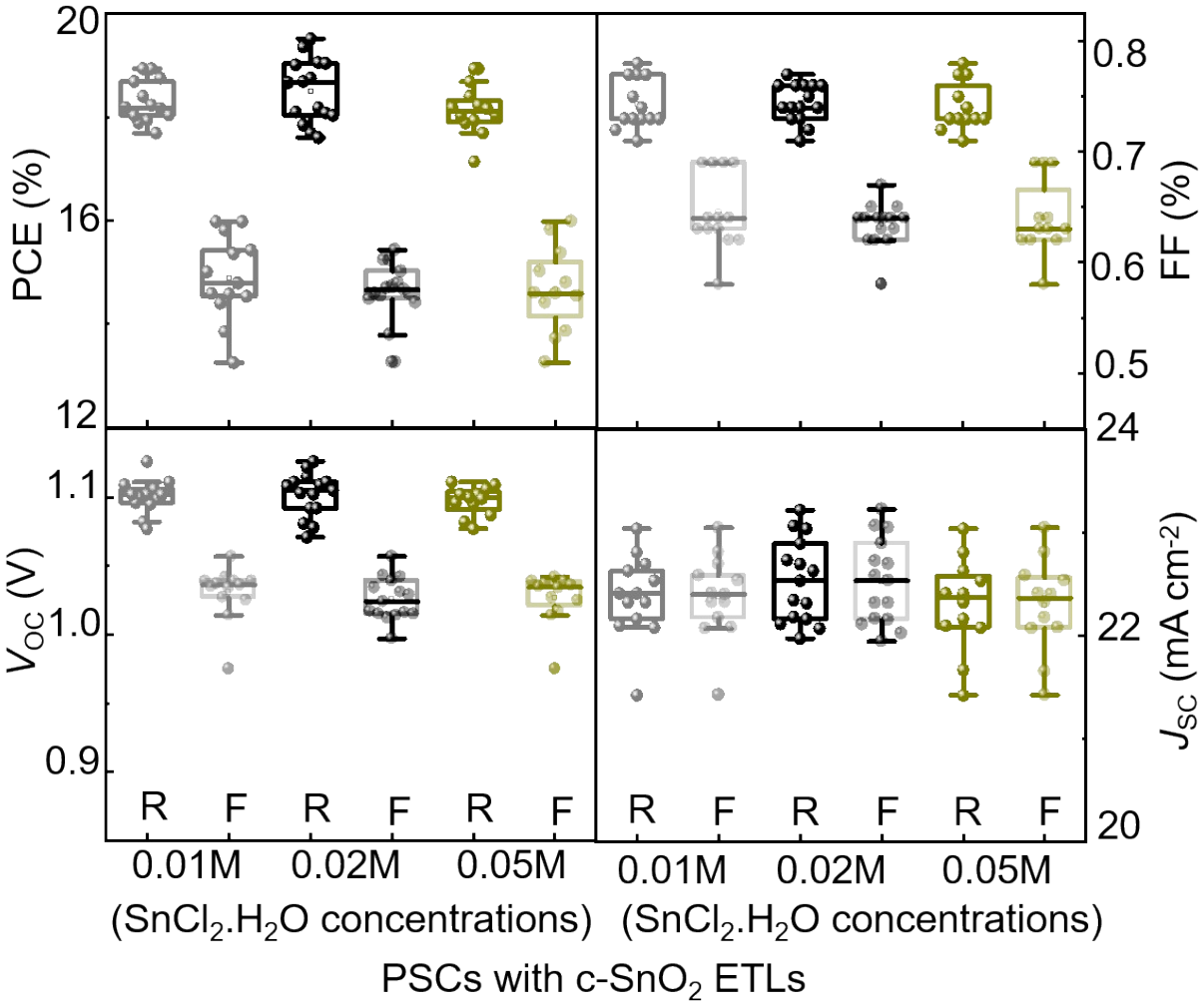

Figure S1. The statistical distribution of photovoltaic parameters of the fabricated PSCs with c-SnO_2 ETLs. The x-axis is the $SnCl_2 \cdot 2H_2O$ solution concentrations.

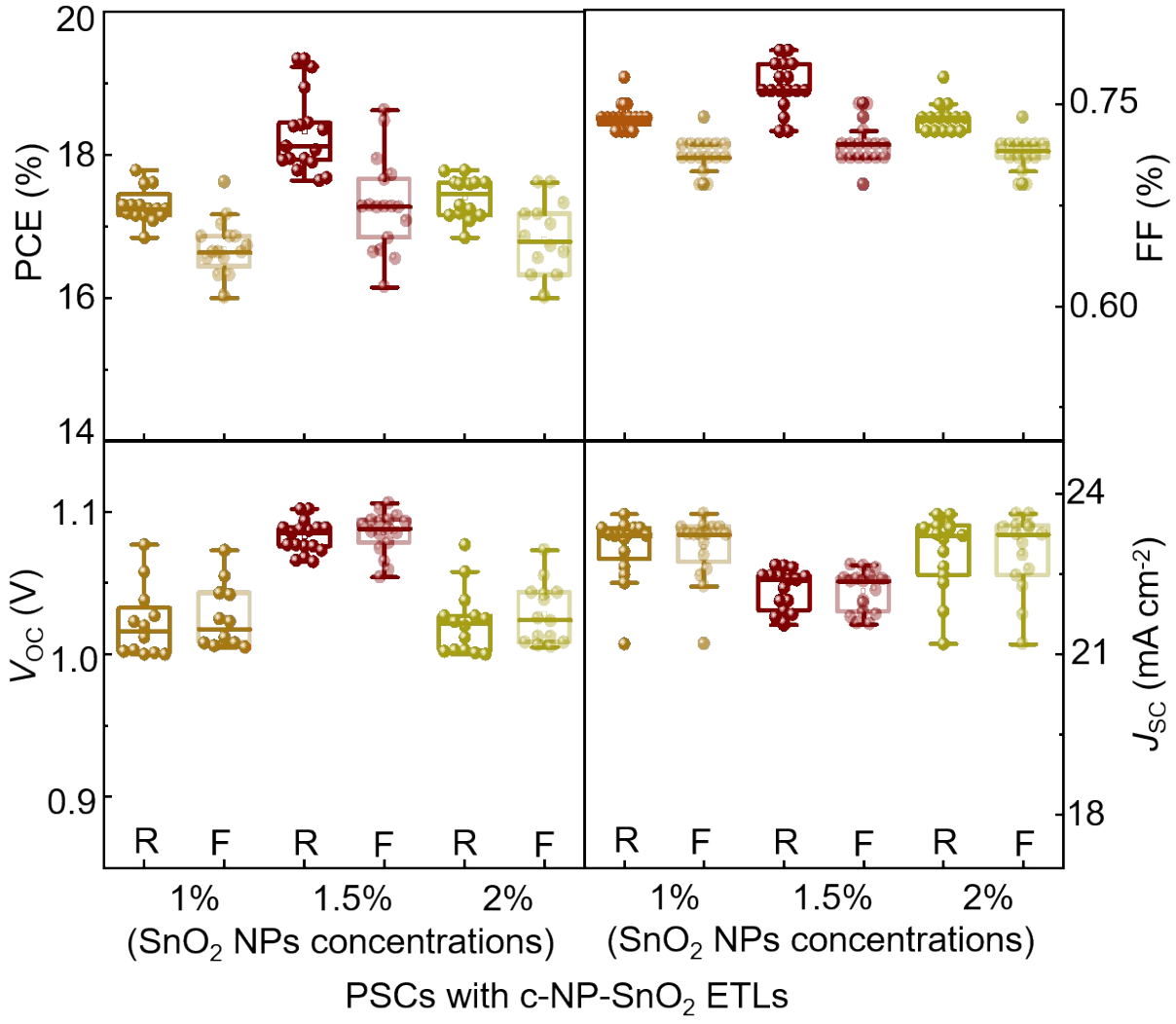

Figure S2. The statistical distribution of photovoltaic parameters of the fabricated PSCs with c-NP-SnO_2 ETLs. The x-axis is the deposited SnO_2 NP_S solution concentrations onto previously optimized c- SnO_2 ETLs.

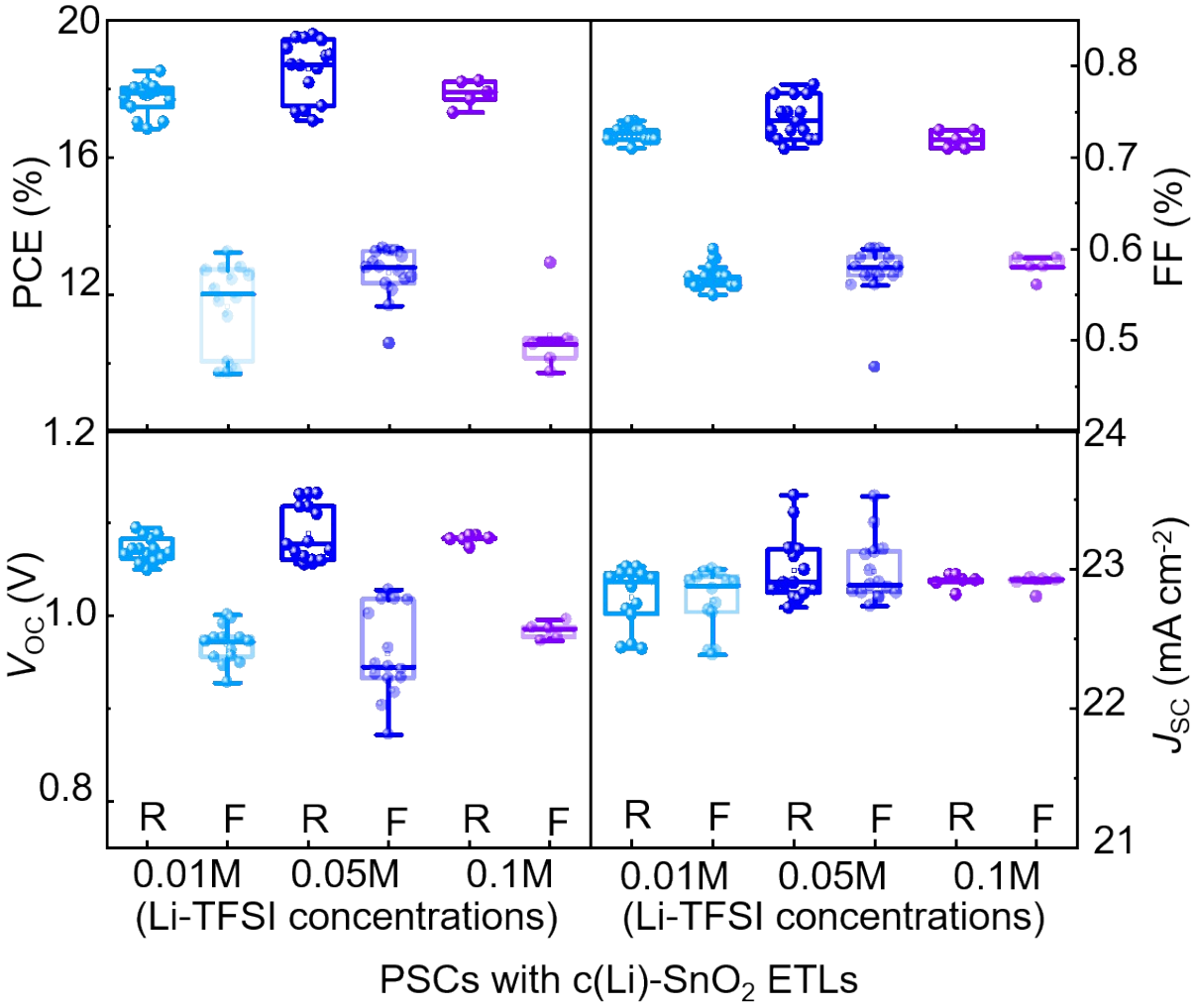

Figure S3. The statistical distribution of photovoltaic parameters of the fabricated PSCs with c(Li)-SnO_2 ETLs. The x axis is the deposited Li-TFSI solution concentrations onto optimum c-SnO_2 layers.

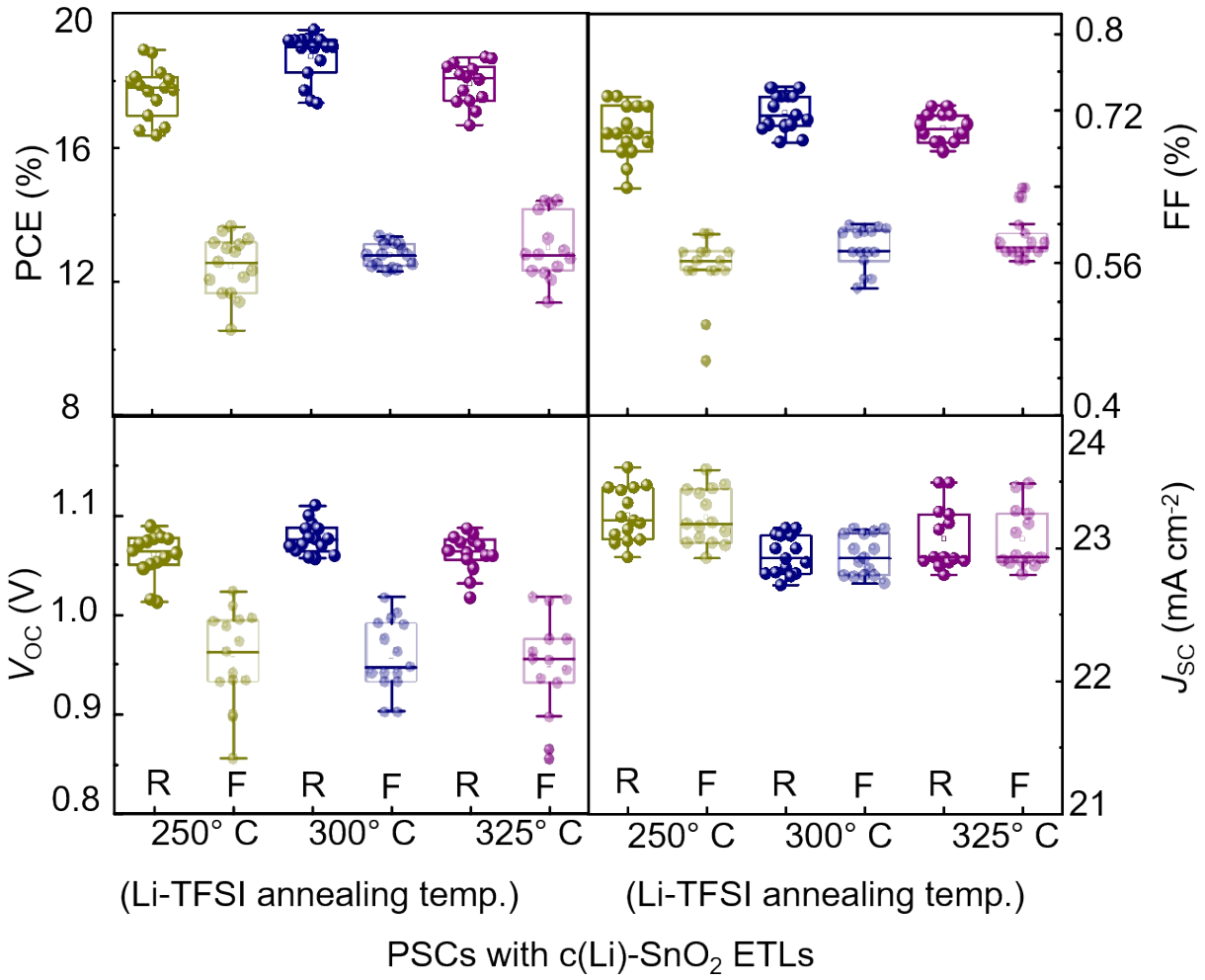

Figure S4. The statistical distribution of photovoltaic parameters of the fabricated PSCs with c(Li)- SnO_2 ETLs, optimizing the Li-TFSI post annealing temperature.

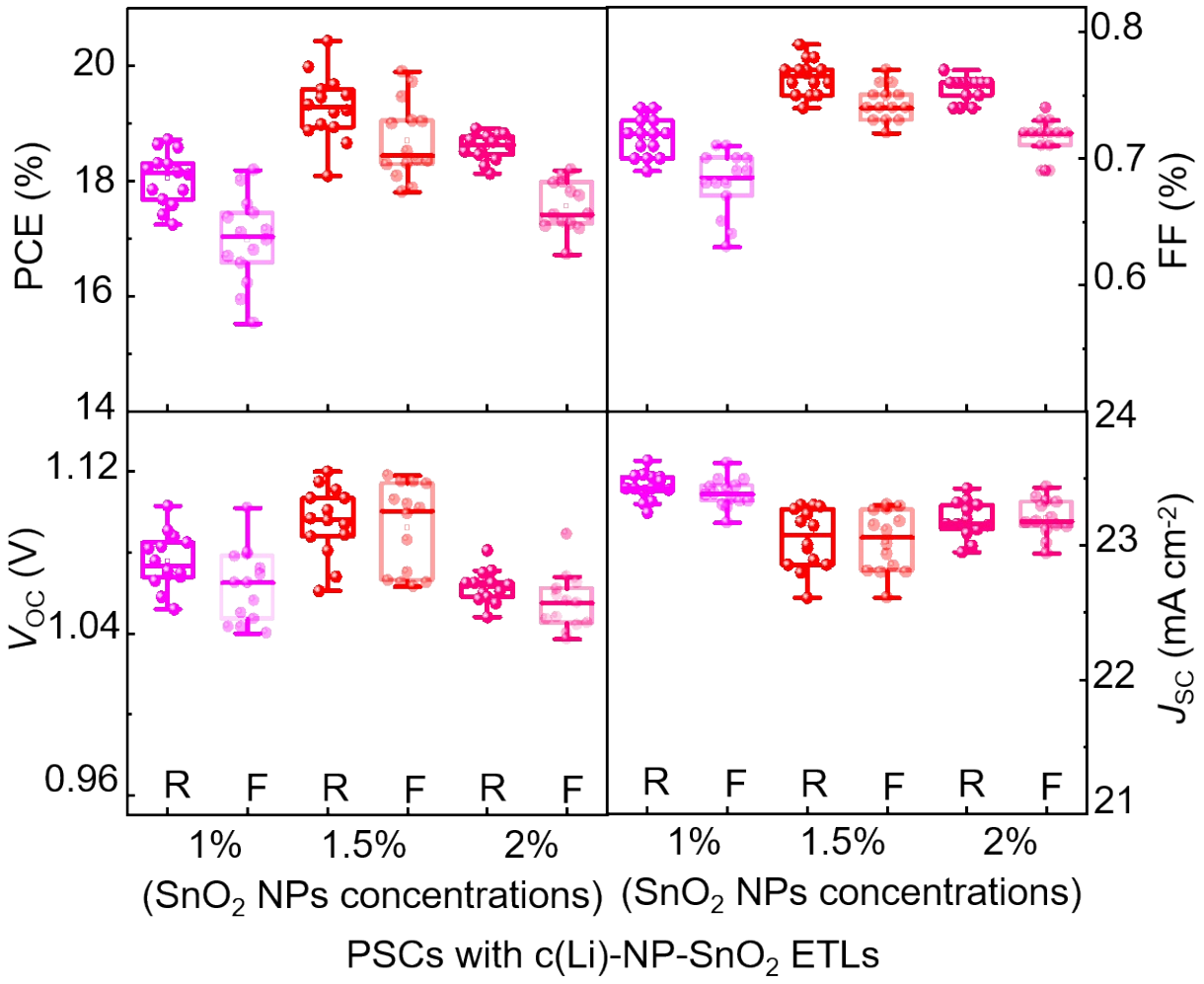

Figure S5. The statistical distribution of photovoltaic parameters of the fabricated PSCs with c(Li)-NP-SnO_2 ETLs. The x axis is the deposited SnO_2 NP_S solution concentrations onto optimum c(Li)-SnO_2 ETLs.

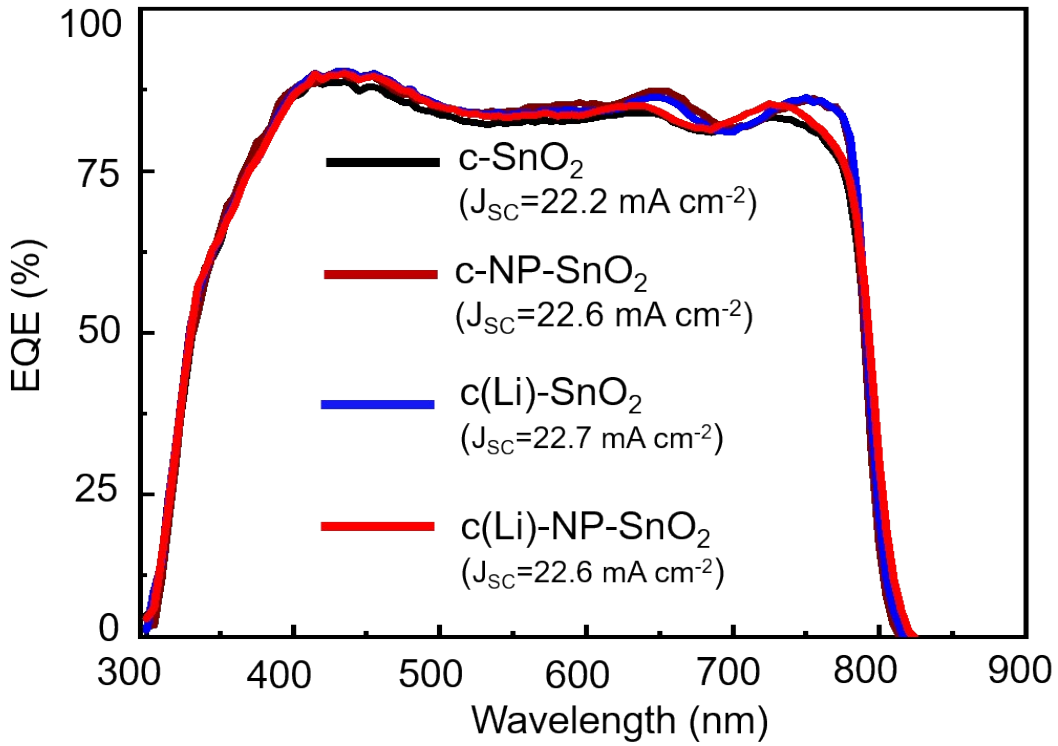

Figure S6. External quantum efficiency (EQE) spectra of PSCs with c-SnO_2, NP-SnO_2, c(Li)-SnO_2, and c(Li)-NP-SnO_2 ETLs.

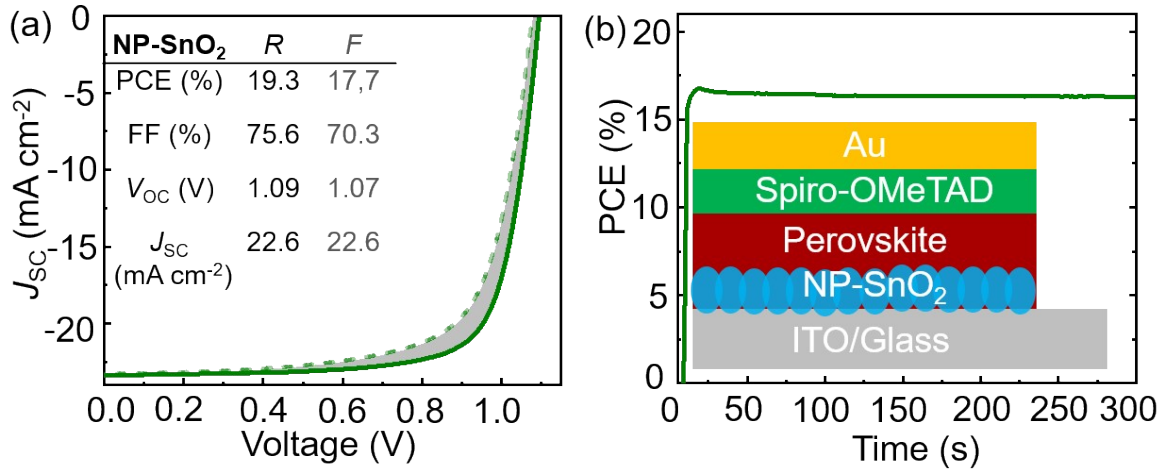

Figure S7. Reverse and forward scan *J–V* characteristics and stabilized PCE under MPP tracking of champion PSC with NP-SnO_2 ETL.

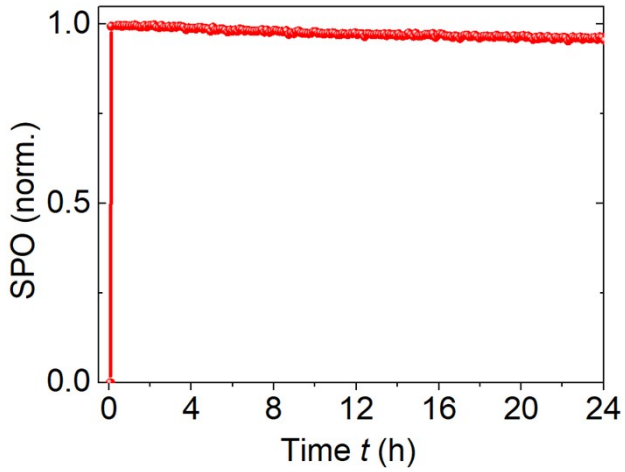

Figure S8. Stabilized power output (SPO) efficiency of the device with c(Li)-NP-SnO2 ETL under one-sun illumination and inert conditions. Data were normalized to the maximum value.

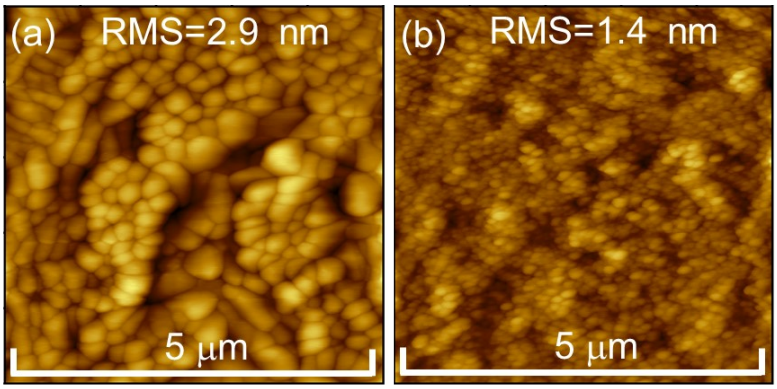

Figure S9. AFM images of (a) a pristine ITO and (b) an ITO/NP-SnO_2 layer.

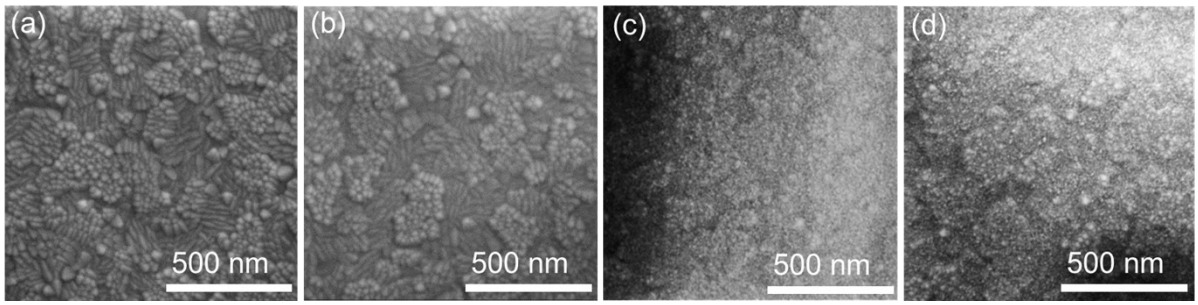

Figure S10. SEM images of the surface morphology of (a) c-SnO_2, (b) c(Li)-SnO_2, (c) c-NP-SnO_2 and (d) c(Li)-NP-SnO_2 ETLs.

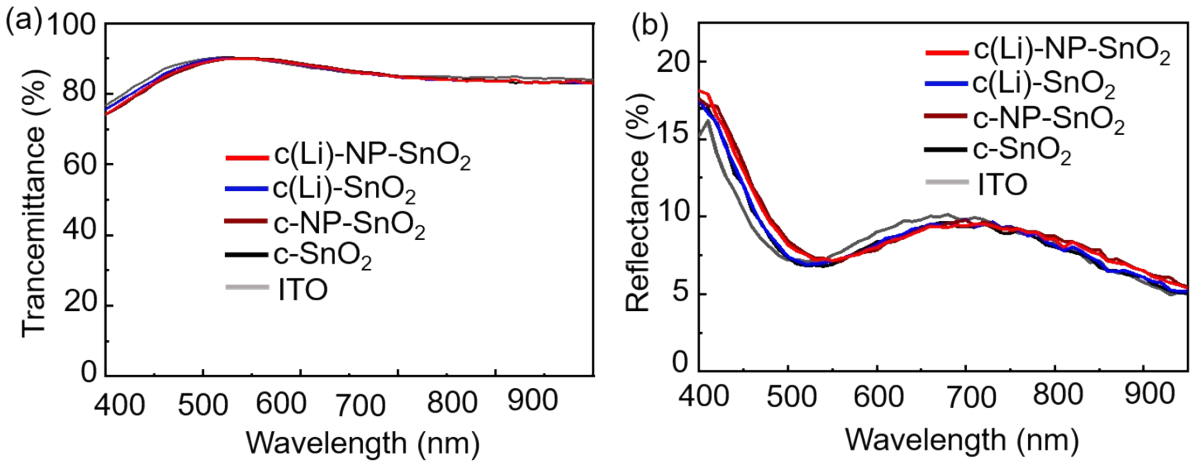

Figure S11. (a) Transmittance and (b) reflectance of ITO, c-SnO_2, c(Li)-SnO_2 and c(Li)-NP-SnO_2 ETLs.

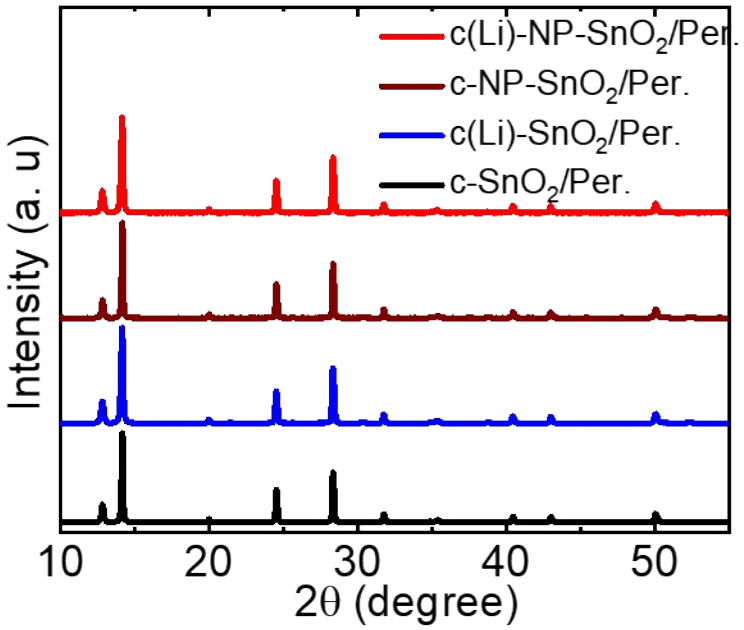

Figure S12. XRD of perovskite thin films deposited on c-SnO_2, c(Li)-SnO_2, c-NP-SnO_2 and c(Li)-NP-SnO_2 ETLs.

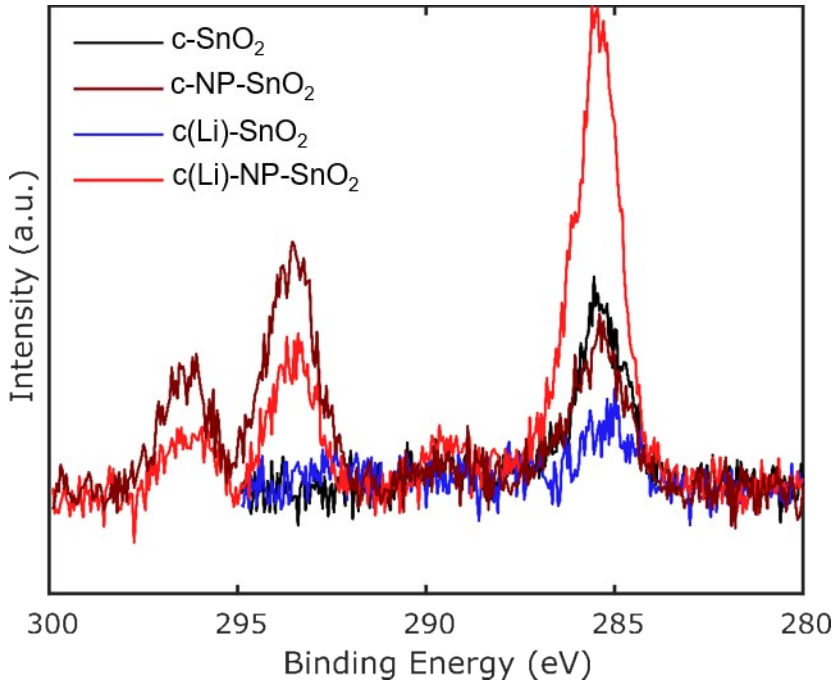

Figure S13. Spectra of the K 2p doublet (293.5 and 296.5 eV) and C 1s (285.5 and 289.5 eV) emissions for the c-SnO_2, NP-SnO_2, c(Li)-SnO_2, and c(Li)-NP-SnO_2 ETLs.

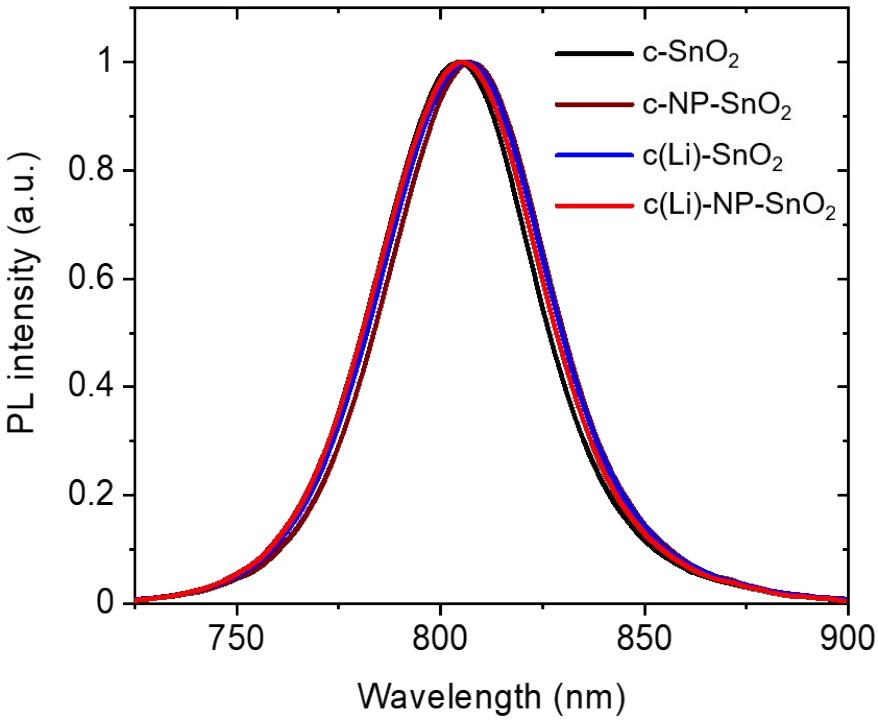

Figure S14. Steady state PL of the fabricated perovskite thin film with c-SnO_2, c(Li)-SnO_2, c-NP-SnO_2 and c(Li)-NP-SnO_2 ETLs.

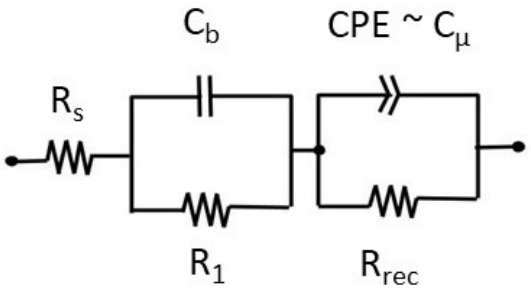

Figure S15. Equivalent circuit used for the EIS data fitting containing constant phase element (CPE).

Table S1. The fitted parameters for the Nyquist plot using equivalent circuit where C_u is calculated as the effective capacitance of CPE part.

Device	R_s (Ω)	R_1 (kΩ)	C_b (nF)	R_{rec} (kΩ)	C_μ (μF)
c-SnO_2	16	2.30	5.82	3.42	65.11
c-NP-SnO_2	19	2.30	6.06	2.83	32.45
c(Li)-SnO_2	15	1.98	6.21	2.32	69.21
c(Li)-NP-SnO_2	15	2.44	5.52	6.51	25.41

Supplementary References

1 J. C. de Mello, H. F. Wittmann and R. H. Friend, *Adv. Mater.*, 1997, **9**, 230–232.

2 L. Krückemeier, U. Rau, M. Stolterfoht and T. Kirchartz, *Adv. Energy Mater.*, 2020, **10**, 1902573.

3 D. A. Shirley, *Phys. Rev. B*, 1972, **5**, 4709–4714.

4 A. Proctor and P. M. A. Sherwood, *Anal. Chem.*, 1982, **54**, 13–19.